Surface Science 103 (1981) 416–430

HARTREE–FOCK–SLATER–LCAO STUDIES OF THE ACETYLENE–TRANSITION METAL INTERACTION
II. Chemisorption on Fe and Cu; cluster models

Petro GEURTS and Ad VAN DER AVOIRD
Institute of Theoretical Chemistry, University of Nijmegen, Toernooiveld, Nijmegen, The Netherlands

Received 2 June 1980; accepted for publication 17 September 1980

Self-consistent Hartree–Fock–Slater–LCAO studies have been performed for (geometrically distorted) C_2H_2 molecules interacting with Fe and Cu clusters of one to three atoms, which model the π, di-σ, μ_2 and μ_3 adsorption sites on Fe(110), (100) and Cu(111), (100) and (110) surfaces. The results have been compared with previous data for Ni surfaces (paper I). Calculated ionization energies are in fair agreement with the measured ones (from UPS): a bonding shift of the acetylene π_u levels, relative to the $3\sigma_g$ level, is found in all cases, but also a larger splitting of these π_u levels occurring on Cu, compared with Fe and Ni. This difference is due to a different C_2H_2–metal interaction: on Fe and Ni we find π to metal donation and (more substantial) metal to π^* back donation, on Cu the first effect is dominated by a strong interaction between the occupied acetylene π_u (and $3\sigma_g$) levels and the filled metal levels which are present in the same energy range (only in Cu, due to the lower lying 3d and 4s bands). This relatively strong (net repulsive) interaction explains the larger π_u level splitting and, also, the observation that C_2H_2 binds weaker to Cu (it desorbs, at higher temperature, and does not dissociate) than to Fe and Ni.

1. Introduction

Although most transition metals can be used as catalysts in some chemical reactions, one finds large differences in activity going along the transition series. These differences appear already in simple processes such as the adsorption of H_2, N_2, NO or CO being molecular on some metals, dissociative on others [1–12]. Also the chemisorption of acetylene, which is interesting for the study of catalytic reactions involving hydrocarbons, shows characteristic differences on Ni, Fe and Cu surfaces. These have been observed under well-defined conditions: single crystal surfaces, rather low temperatures and low coverages (less than a monolayer).

On the Ni(111) surface C_2H_2 is adsorbed molecularly at $T \simeq 100$ K [13–18]. At higher temperatures (300 to 400 K) the molecules dissociate into CH fragments [14,19,20]. Also on the Ni(100) and (110) planes molecular C_2H_2 adsorption has been observed at low temperature [16,21]. For Fe, which has a more open bcc

lattice (whereas Ni and Cu have the closest packed fcc structure), the activity of the low index planes seems to depend on the packing density. On the densest Fe surface, (110), molecular C_2H_2 adsorption occurs without fragmentation, at temperatures up to 300 K, according to UPS (ultraviolet photoelectron spectroscopy) [7], LEED (low energy electron diffraction) [11] and thermal desorption [11] studies. On the most open low index plane, (111), adsorption is mainly [11] or completely [22] dissociative (at 300 K) with both C–C and C–H bonds breaking. The medium density (100) face adsorbs C_2H_2 at 98 K, first molecularly, and then gradually converts it into fragments [23] (this process is enhanced by raising the temperature to 123 K). If this (100) surface is partially deactivated by preadsorption of carbon or oxygen, adsorbed C_2H_2 remains molecular. Also on polycrystalline Fe films molecular C_2H_2 adsorption has been observed at low temperature (110 K) [24]. On Cu surfaces the situation is rather different. Both, on Cu(100) faces [15] and on polycrystalline Cu films [24], C_2H_2 is molecularly adsorbed from 80 to 300 K. At higher temperatures C_2H_2 desorbs reversibly without any decomposition taking place. So, on the whole, we can conclude that molecular C_2H_2 adsorption is probably weaker on Cu than on Fe and Ni. Whereas the latter two metals can split C_2H_2 into (adsorbed) fragments, Cu cannot. The activity of the Fe and Ni surfaces seems to be highest for the most open (Fe) surfaces. Also stepped Ni surfaces can dissociate C_2H_2 (into C_2 fragments) at low temperature (150 K) [20,25].

These observations, and the available structural (LEED [11,14,26–28]) and spectroscopic data (UPS spectra for C_2H_2 on Fe, Ni and Cu [7,13–16,21–24,29], ELS spectra for the Ni(111) surface [17–20,25,30]) form an interesting basis for theoretical studies. We have investigated already (see paper I in this series [31]) the molecularly adsorbed state of C_2H_2 on Ni surfaces (mainly the (111) surface, since most experimental information is available there). We have done this by means of self-consistent Hartree–Fock–Slater–LCAO calculations of C_2H_2 interacting with small clusters of Ni atoms which represent the different adsorption sites on the surface. By extending these calculations to Fe and Cu clusters we want to throw some light on the observed activity differences and to explain the differences in the UPS spectra as well.

Other studies which are related to these problems are semi-empirical (Extended Hückel) calculations for C_2H_2 on Fe clusters [32,33] and ab initio Hartree–Fock–LCAO calculations for (geometrically distorted) C_2H_2 (free or bonded to a Be atom) [15,16,34] and C_2H_2 interacting with one Fe or Cu atom [35]. We think that additional insight can still be gained from further systematic theoretical work, however (as we have explained in paper I).

2. Method and calculations

The non-empirical (spin-restricted) Hartree–Fock–Slater (HFS)–LCAO method used has been described in detail elsewhere [36–38] and, briefly, in paper I. The

atomic orbital basis set (double zeta Slater type orbitals [39]) and the density fit functions have been chosen as in I: 3d, 4s and 4p orbitals on Fe (from the $3d^6 4s^2$ ^5D state) and Cu (from the $3d^{10} 4s^1$ ^2S state), 2s and 2p on C and 1s on H and fit functions up to g-type inclusive. The core electrons have been replaced by a non-empirical pseudo-potential [40].

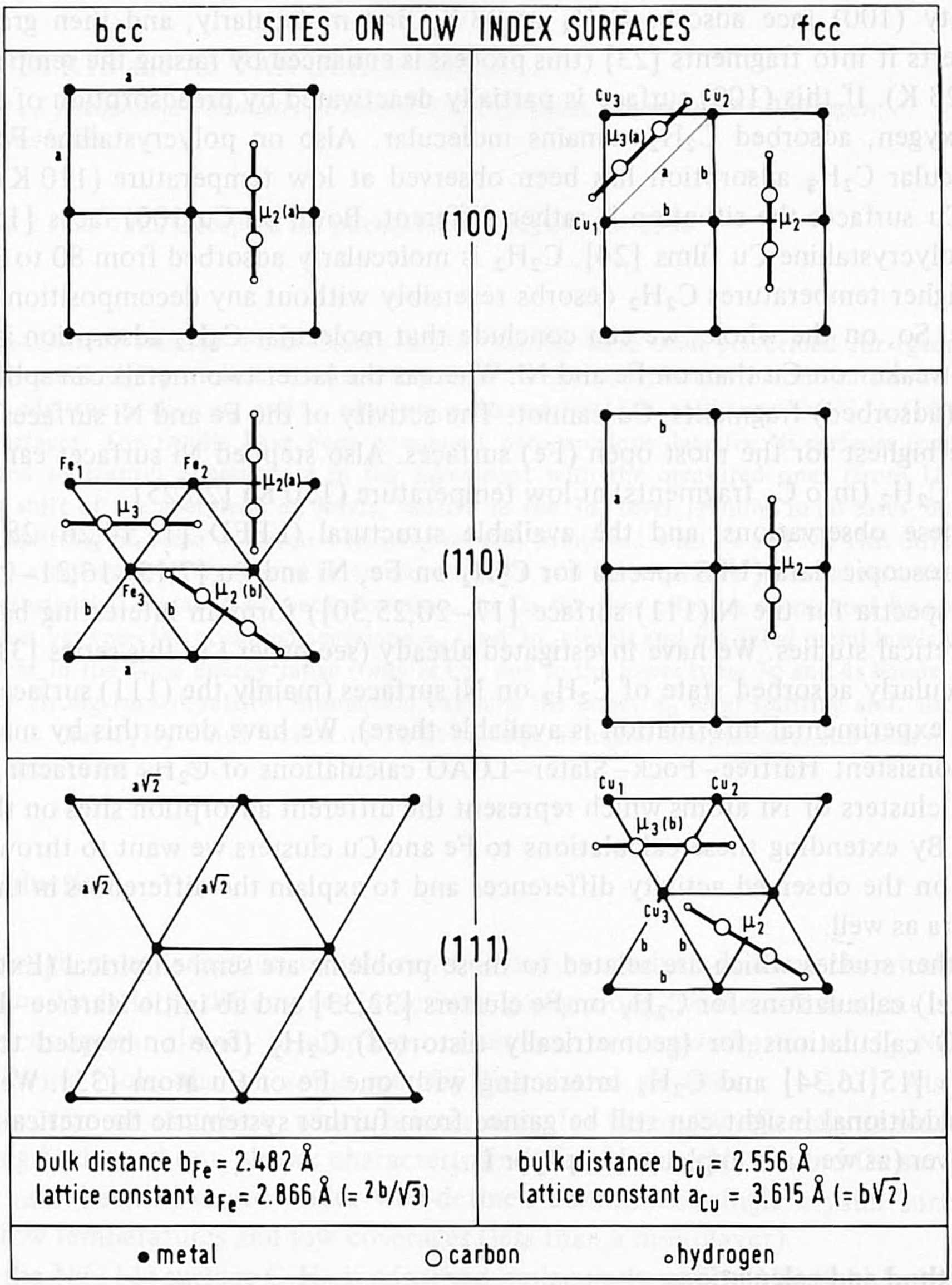

Fig. 1. Structures (drawn to scale) of low index surfaces (100), (110) and (111) of bcc iron and fcc copper (bulk nearest neighbour distances, b_{Fe} and b_{Cu}, from ref. [41]). The (projected) positions of C_2H_2 (distorted, CCH angle 150°) for the μ_2 and μ_3 sites have been indicated too.

The structures of the three low index surfaces of bcc Fe and fcc Cu (and Ni) are depicted in fig. 1. Just as for C_2H_2 on Ni we have studied π bonding (C_2H_2 on top of one metal atom), di-σ bonding (C_2H_2 bridging over 2 metal atoms with the C–C axis parallel to the metal–metal axis), μ_2 bonding (a double π bond, with two metal atoms) and μ_3 bonding (a π bond with one metal atom and a di-σ bond with two others), see also fig. 1. So, our metal clusters range from one to three atoms. The cluster models for C_2H_2 adsorption on Cu are the same as for Ni (see paper I, fig. 1), but the metal–metal nearest neighbour distance $b_{Cu} = 2.556$ Å [41] is somewhat larger ($b_{Ni} = 2.492$ Å [41]) and, moreover, we have also considered a μ_3 site, $\mu_3(a)$, which occurs on the Cu(100) surface (for which surface the UPS spectrum has been measured). The distance between two of the metal atoms is equal to $a = b\sqrt{2}$ in this case (see fig. 1). For Fe, which has a different lattice structure (bcc) with a slightly smaller neighbour distance $b_{Fe} = 2.482$ Å [41], the μ_3 site occurring on the densest plane (110) is somewhat different, too (see fig. 1). The di-σ and μ_2 sites have been studied for two metal–metal distances, b and $a = 2b/\sqrt{3}$ (clusters denoted by di-$\sigma(b)$, $\mu_2(b)$ and di-$\sigma(a)$, $\mu_2(a)$, respectively). Clusters with larger metal–metal distances (e.g. $a\sqrt{2}$) have not been studied since the more open Fe surface (111) does not seem to adsorb C_2H_2 molecularly.

In all models the C–C axis is kept parallel to the "surface" with a carbon to metal (internuclear) distance of 1.9 Å. The adsorbed acetylene molecule is distorted from the linear structure by bending the CH bonds over 30° (in the vertical plane) and, at the same time, using C–C and C–H bond lengths which are intermediate between the values of free acetylene [41] and those of ethylene [42]. This structure with a CCH angle close to 150° and a metal–carbon distance of 1.9 Å has been found as the most probable one in our studies (paper I) for C_2H_2 adsorption on Ni(111); it is in agreement with the X-ray structures of alkyne–transition metal complexes [43–57]. For the π site on Fe surfaces we have considered the linear and the 60° bent C_2H_2 structures, too ($\angle_{CCH} = 180°$ and 120°, respectively). The structural parameters for the adsorption clusters are the same as in our study of C_2H_2 on Ni (except of course the metal–metal distances), see paper I, fig. 1.

The analysis of the results proceeds along the same lines as in paper I. We could not use the total (adsorption) energies since they are not sufficiently accurate in these large systems for looking at the subtle differences we are interested in (e.g. the relative stability of different adsorption sites). As mentioned in paper I, this is due to the numerical integration method; work on this problem is still in progress. Instead, the measured adsorption shifts in the UPS spectrum of C_2H_2 are compared with the shifts in the ionization energies calculated for the cluster models. The latter values are calculated within the HFS formalism in most cases by the transition state method [37,58]. Also the calculated (relative) level positions from ground state HFS calculations can be used, however, since the relaxation effects on the electron binding energies are practically uniform for the upper valence levels of C_2H_2 [31]. The bonding of C_2H_2 to Fe and Cu clusters is discussed, both by looking at the level (bonding/anti-bonding) shifts and at the character of the molecular

orbitals involved. This character is expressed by a Mulliken population analysis [59,60] in terms of the atomic orbitals, but also in terms of the MO's of acetylene * (after a linear transformation). By the latter results we can quantify the Dewar–Chatt–Duncanson donation–back donation effects [61,62]. The data are compared with the Ni results (paper I), but, unfortunately, no ELS spectra are available for C_2H_2 on Fe and Cu.

3. Results

3.1. Adsorption of C_2H_2 on Fe

The UPS spectrum for C_2H_2 adsorbed on Fe surfaces is similar to the spectrum for Ni surfaces: the π_u levels have a bonding shift relative to the $3\sigma_g$ level, the $2\sigma_u$–$3\sigma_g$ splitting remains almost constant, see figs. 2, 3. This π_u bonding shift is largest for Fe films [24], it is still considerable for the (110) surface [7] but it becomes very small for (100) [23]. On the latter surface, however, the UPS spectrum must be measured immediately after adsorption or on a partially deactivated surface (precovered with carbon or oxygen), since otherwise C_2H_2 becomes dissociated. Only a single π_u peak is observed in the spectra, indicating that the splitting between the two π_u levels should not be too large (smaller than 1 eV probably).

Figs. 2 and 3 also display the calculated adsorption shifts in the electron binding energies for C_2H_2 on Fe clusters. The levels shown are the only ones which are predominantly composed of the occupied C_2H_2 valence levels; they are the lowest valence levels in the C_2H_2–Fe clusters (the same as for Ni, cf. paper I). Only the results for the di-$\sigma(b)$ and $\mu_2(b)$ clusters (see section 2) have been indicated, since those for di-$\sigma(a)$ and $\mu_2(a)$ do not differ significantly. (Note that the Fe–C distances are always 1.9 Å, so that for the (a) clusters, with the larger Fe–Fe distance, the C_2H_2 molecule is somewhat closer to the "surface".)

The calculated shifts for the μ_2 and μ_3 adsorption clusters are in agreement with the observed UPS spectra. For di-σ bonding the $\pi_\perp$–$\pi_{/\!/}$ splitting becomes too large; this is true also for π bonding, but only in the transition state results. Except for this latter case which is exceptional (we shall discuss it below), the transition state results lead to practically the same shifts of the upper C_2H_2 valence levels as the ground state results, indicating a uniform relaxation effect for these levels. Only the lowest C_2H_2 valence level ($2\sigma_g$) shows a larger relaxation shift (cf. also paper I), but the position of this level has not been measured on Fe surfaces (neither on Cu). The very small π_u bonding shift measured for the (100) surface is not found in any of

* We use the free acetylene MO nomenclature (σ_g, σ_u, π_u, π_g^*) also for the MO's in the cluster models; actually, the symmetry is lowered, of course. By $\pi_\perp$ and $\pi_{/\!/}$ we denote π orbitals perpendicular and parallel to the "surface", respectively.

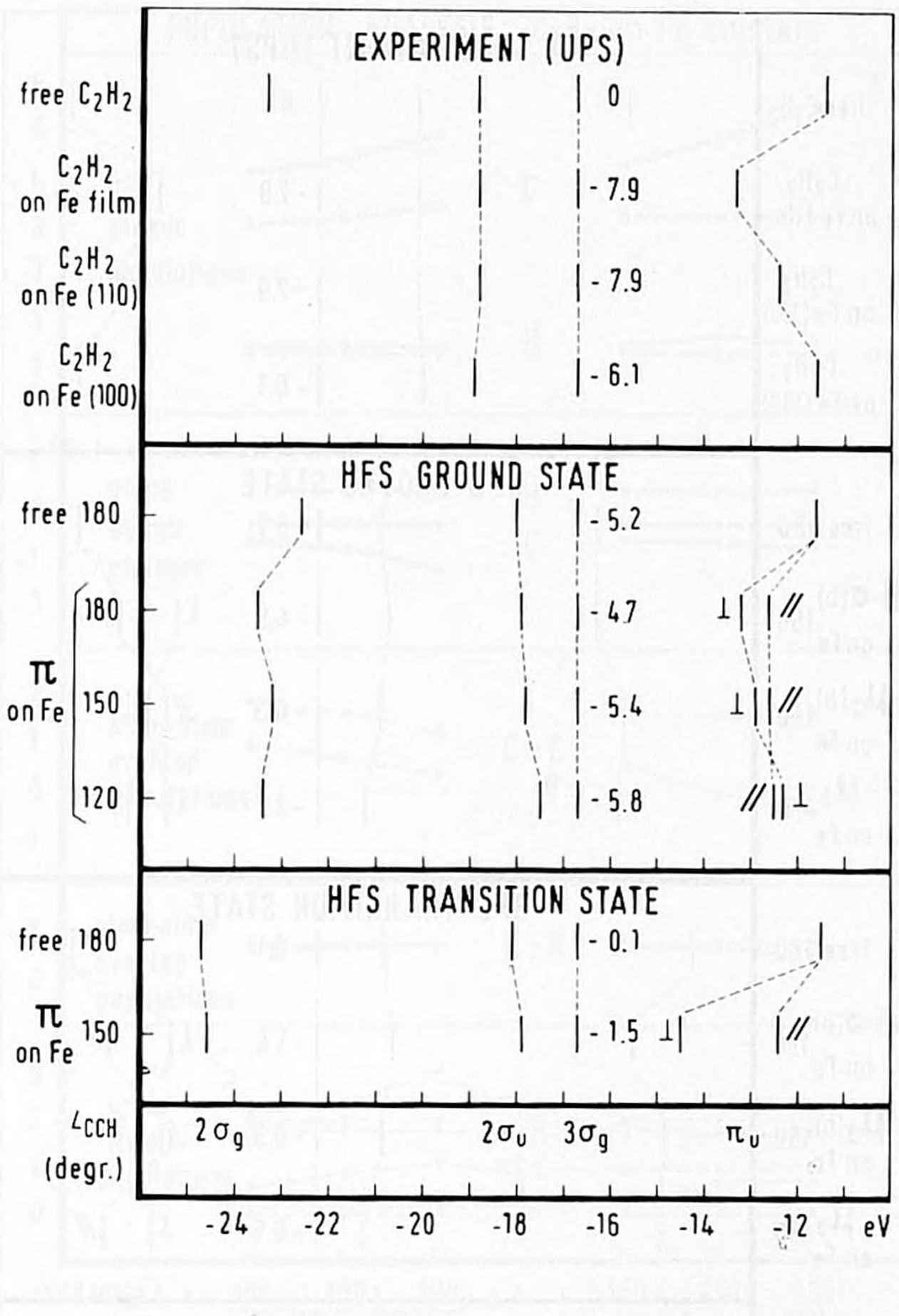

Fig. 2. MO schemes for C_2H_2 on the Fe π site from HFS ground state and transition state calculations, compared with the free C_2H_2 level scheme [31]. The same comparison is indicated for the experimental (UPS) ionization energies of C_2H_2 molecularly adsorbed on an Fe film [24], on Fe(110) [7] and on Fe(100) [23] (all measured relative to the work function) and the ionization energies of free C_2H_2 [16,63]. All spectra have been shifted by the amount indicated (in eV) next to the $3\sigma_g$ levels in order to bring these $3\sigma_g$ levels into the same position.

the cluster models. The molecularly adsorbed C_2H_2, which is not stable on this surface and possibly bound weaker [23,33], might occupy a position (farther away from the surface?) which is not represented by our models.

Let us now look at the electronic charge distribution in the clusters. The Mulliken populations on the adsorbed C_2H_2 molecules are shown in fig. 4, see also table 1; the $2\sigma_g$, $2\sigma_u$ and $3\sigma_g$ populations remain practically equal to two. Generally the results are very similar to the Ni results (paper I). There is some donation of acetylene π_u electrons to the metal and a more substantial back-donation of metal electrons to the anti-bonding π_g^* orbitals. The combination of these two effects leads to

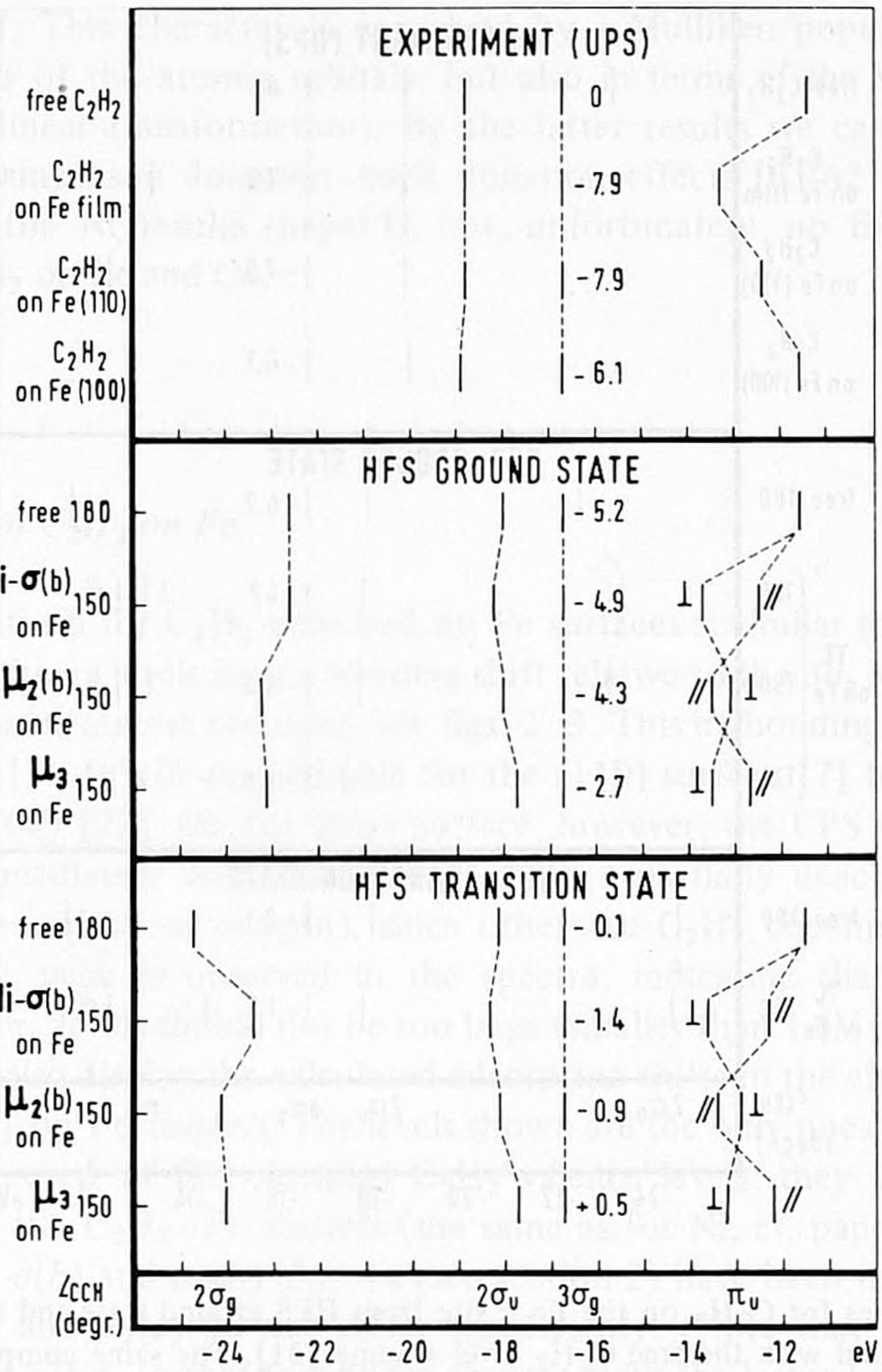

Fig. 3. MO schemes for C_2H_2 on the Fe_2 di-$\sigma(b)$ and $\mu_2(b)$ sites and on the Fe_3 μ_3 site; see further the caption of fig. 2.

a considerable decrease in the C–C overlap population, a growth of the C net atomic population and an increased negative charge on C. The magnitude of these effects increases in the order $\pi < \text{di-}\sigma < \mu_2 < \mu_3$ just as for Ni; in the μ_2 and μ_3 cases both the $\pi_\perp$ and the $\pi_{/\!/}$ orbitals of C_2H_2 become involved (see paper I) and this should lead to a considerable decrease in the C–C bond strength. (For Ni [31] this has been compared with the shift in the C–C stretch frequency as measured by ELS [17,18,30].) We have also found some differences with the Ni results, however. The first one is that the lowering in the C–C overlap population (and thus, probably, in the C–C stretch frequency [31,64,65], which has not been measured for Fe, however) for the μ_3 site on the Fe(110) surface is slightly less than for the μ_3 site on Ni(111). (Also the π_u and $2\sigma_g$ bonding shifts are somewhat smaller.) This is under-

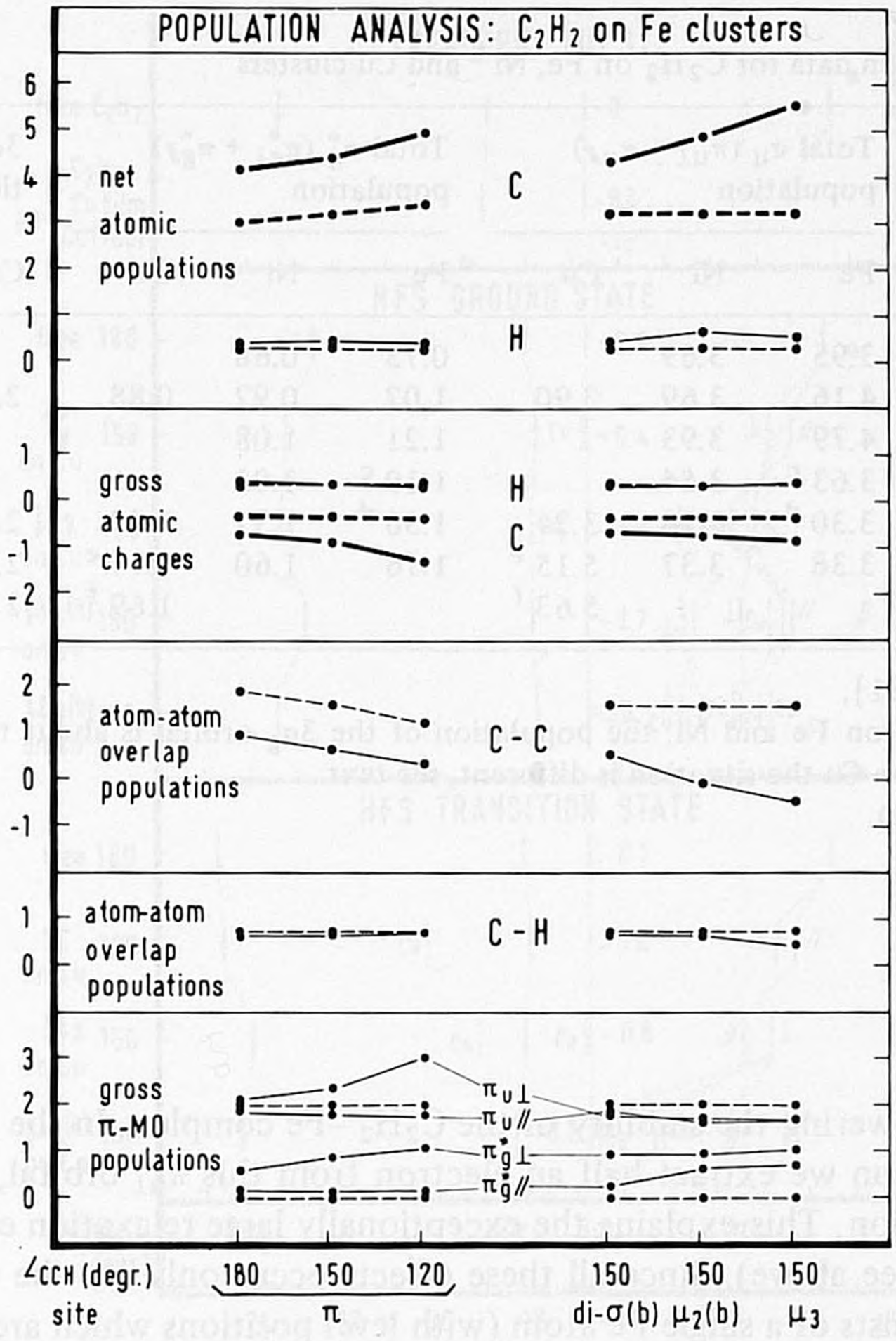

Fig. 4. Population analysis data for C_2H_2 on the various Fe sites (———), compared with free C_2H_2 results [31] (– – –).

standable when one realizes that for the μ_3 site on Fe(110) two Fe atoms have a somewhat larger distance ($a = 2b/\sqrt{3}$, see fig. 1). Consequently, the difference in interaction strength between the μ_2 and μ_3 sites (although we do not know the interaction energies) seems somewhat smaller on Fe(110) than on Ni(111).

The second difference concerns the π site which yields a somewhat peculiar behaviour for Fe. The Mulliken population of the acetylene $\pi_{u\perp}$ orbital is larger than two, see table 1. Although such a result (which we shall encounter for Cu also) has no direct physical interpretation (it is due to the definition of the Mulliken populations), it points to a specific type of interactions occurring. In this case, it is caused by an occupied Fe orbital which lies only slightly above the occupied acetylene $\pi_{u\perp}$ orbital; these orbitals, which have the same symmetry, strongly interact. Since both orbitals are doubly occupied the net interaction will

Table 1
Selected population data for C_2H_2 on Fe, Ni [a] and Cu clusters

Site	$\angle_{CCH}$ (deg)	Total π_u ($\pi_{u\perp} + \pi_{u\parallel}$) population			Total π_g^* ($\pi_{g\perp}^* + \pi_{g\parallel}^*$) population			$3\sigma_g$ population [b]
		Fe	Ni	Cu	Fe	Ni	Cu	Cu
	180	3.95	3.69		0.75	0.68		
π	150	4.16	3.69	3.90	1.02	0.92	0.88	2.56
	120	4.79	3.93		1.21	1.08		
di-σ	150	3.63 [c]	3.54		1.19 [c]	1.02		
μ_2	150	3.30 [d]	3.34	3.24	1.56 [d]	1.37	1.39	2.59
μ_3	150	3.38	3.37	5.15 [e]	1.76	1.60	1.74 [e]	2.01 [e]
				5.63 [f]			1.69 [f]	2.03 [f]

[a] From paper I [31],
[b] For adsorption on Fe and Ni, the population of the $3\sigma_g$ orbital is about two (see text and paper I [31]); on Cu the situation is different, see text.
[c] Value for di-$\sigma(b)$.
[d] Value for $\mu_2(b)$.
[e] Value for $\mu_3(b)$.
[f] Value for $\mu_3(a)$.

be repulsive, lowering the stability of the C_2H_2–Fe complex. In the transition state for $\pi_{u\perp}$ ionization we extract half an electron from this $\pi_{u\perp}$ orbital, which leads to extra stabilization. This explains the exceptionally large relaxation effect found for the $\pi_{u\perp}$ level (see above). Since all these effects occur only for the π site iron cluster, which consists of a single Fe atom (with level positions which are unrealistic for the metal), we shall not attempt to attribute any physical reality to them in this case. Moreover, it is not very probable in view of our findings, that the π site is preferred by C_2H_2 adsorbing on Fe surfaces.

3.2. Adsorption of C_2H_2 on Cu

In some aspects the UPS spectrum for C_2H_2 on Cu surfaces [15,24], see fig. 5, resembles the spectra for Ni and Fe surfaces: one has observed a bonding shift of the acetylene π_u levels relative to the $3\sigma_g$ level and practically no change in the $2\sigma_u$–$3\sigma_g$ splitting. For Cu, both on the (100) surface [15] and on polycrystalline films [24] one has found a distinct splitting of the acetylene π_u levels, however, which does not occur for Ni and Fe. We compare these results in fig. 5 with the ionization energy shifts calculated for C_2H_2 interacting with the Cu clusters.

The calculated results are rather different from the Ni and Fe results. For Ni and Fe we have found a set of orbitals in the C_2H_2–metal clusters (the lowest valence orbitals) which are in one to one relation with the occupied acetylene valence orbi-

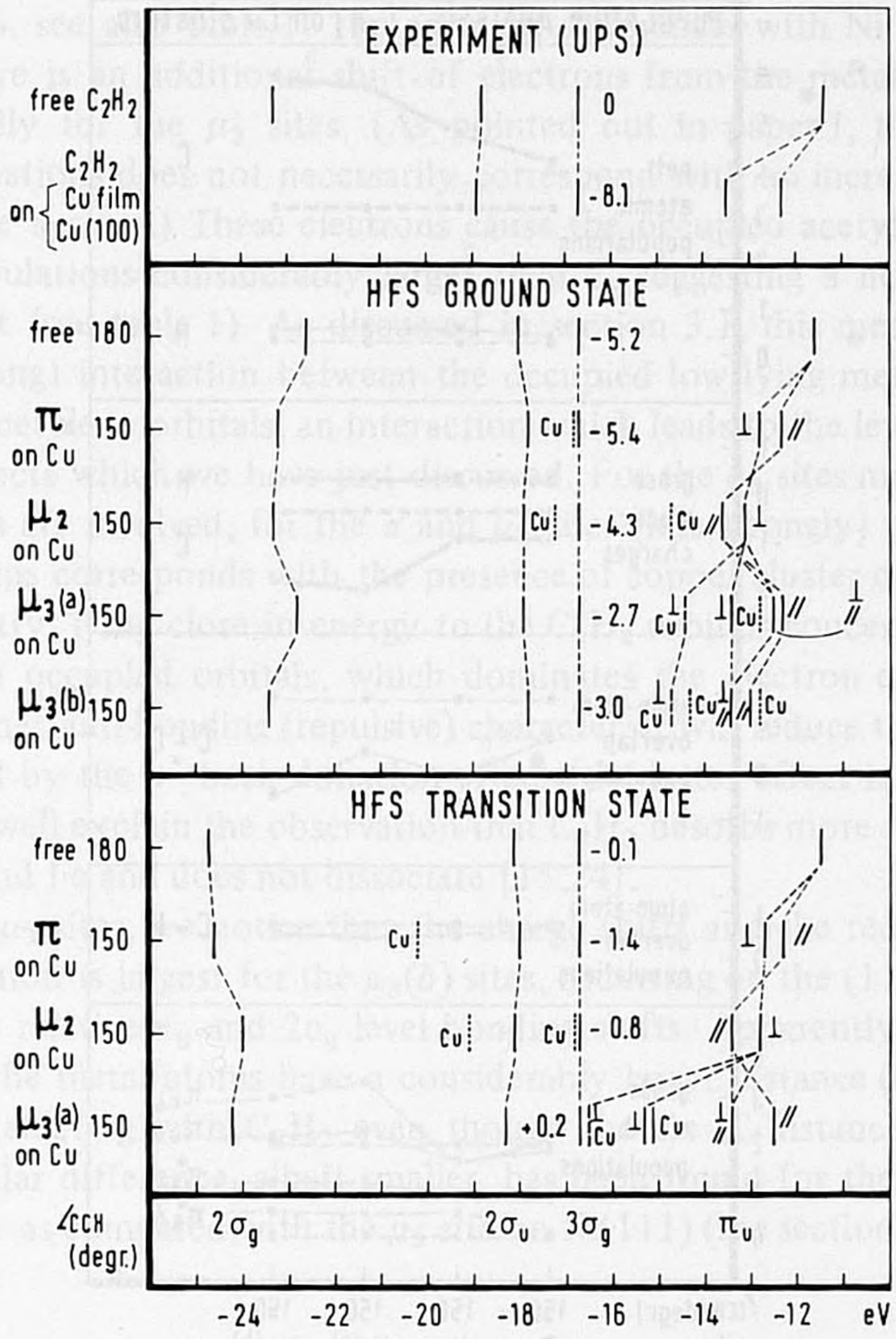

Fig. 5. MO schemes for C_2H_2 on the Cu π site, the Cu_2 μ_2 site and the Cu_3 $\mu_3(a)$ and $\mu_3(b)$ sites from HFS ground state and transition state calculations, compared with the free C_2H_2 level scheme [31]. The same comparison is indicated for the experimental (UPS) ionization energies of C_2H_2 molecularly adsorbed on a Cu film [24] and on Cu(100) [15] (coinciding in the figure; both are measured relative to the work function) and the ionization energies of free C_2H_2 [16,63]. All spectra have been shifted by the amount indicated (in eV) next to the $3\sigma_g$ levels in order to bring these $3\sigma_g$ levels into the same position. Dotted bars (with the symbol Cu) represent almost pure Cu levels; dashed bars labelled by $\frac{\perp}{Cu}$ stand for about equal mixtures of $\pi_{u\perp}$ and Cu orbitals; levels indicated by $\frac{\perp}{/\!/}$ have about equal $\pi_{u\perp}$ and $\pi_{u/\!/}$ character. Furthermore on the μ_3 sites, all π_u orbitals have small admixtures of Cu character.

tals; each of these cluster MO's contains one C_2H_2 valence MO with large weight. For Cu we notice (in fig. 5) that almost pure Cu MO's are lying lower than the highest valence levels of C_2H_2, but also that some of the occupied C_2H_2–Cu cluster MO's consist of both C_2H_2 and Cu orbitals in different admixtures. Moreover, the acetylene orbitals $\pi_{u\perp}$, $\pi_{u/\!/}$ and (somewhat less) $3\sigma_g$ are mixed among themselves.

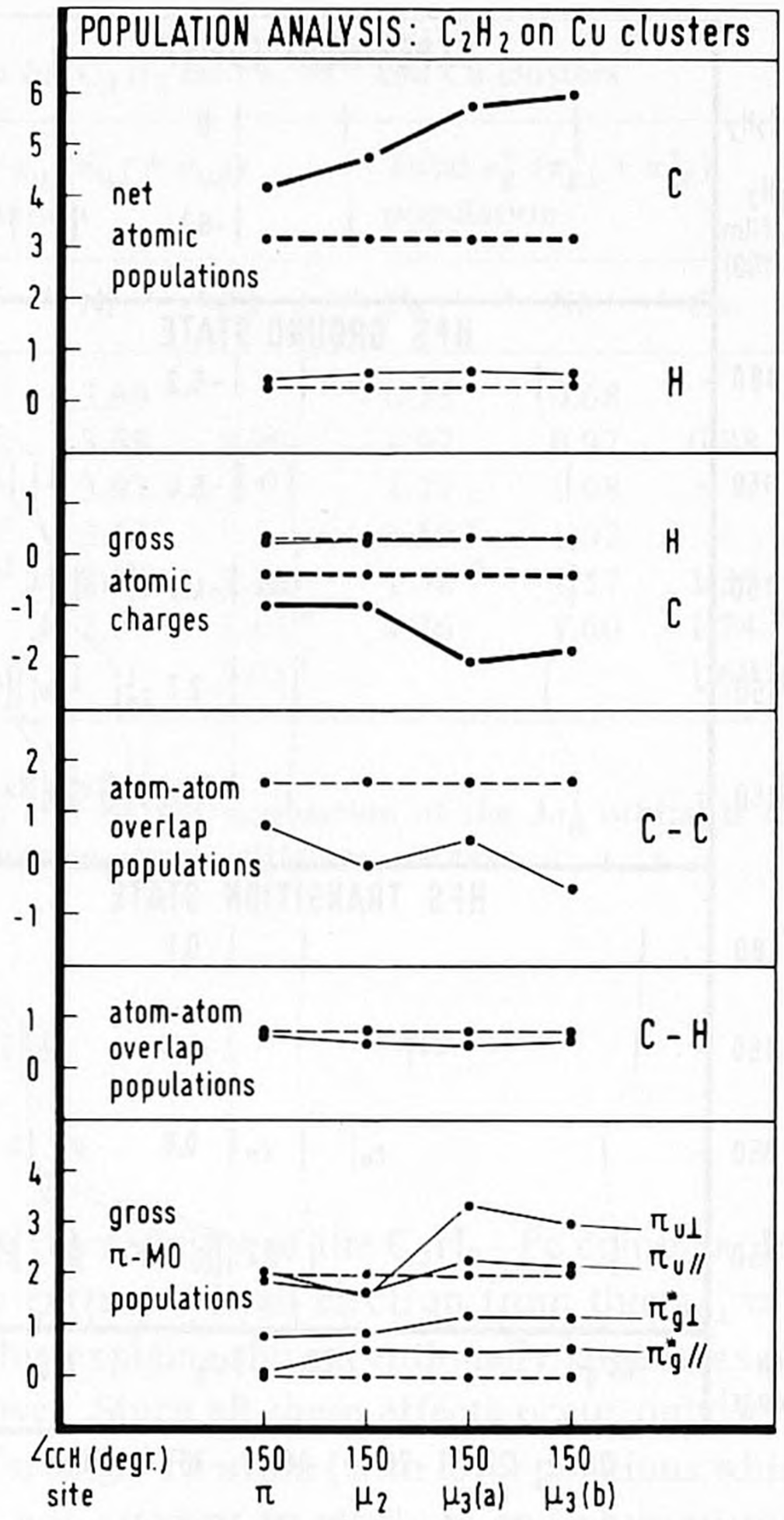

Fig. 6. Population analysis data for C_2H_2 on the various Cu sites (———), compared with free C_2H_2 results [31] (– – –).

This strong interaction with the (occupied) low lying Cu orbitals leads to a splitting (and, on the real surface, probably broadening) of the acetylene π_u levels on the larger (tri-atomic) μ_3 clusters, in addition to the (smaller) $\pi_\perp$–$\pi_{//}$ splitting observed on Ni and Fe. This can explain the finding of two (π) peaks in the UPS spectrum of C_2H_2 on Cu, whereas there is only one on Ni and Fe. The bonding shift of these (mainly) π_u levels relative to the $3\sigma_g$ level and the small change of the $2\sigma_u$–$3\sigma_g$ splitting also emerge from the calculations. Finally, we note that the bonding shift of the acetylene π_u levels (and of the $2\sigma_g$ level, which has not been measured on Cu, however) is smaller for the $\mu_3(a)$ site occurring on the (100) face than for the $\mu_3(b)$ site on (111).

Let us now look at the population analysis again. Most of the acetylene data are

shown in fig. 6, see also table 1. The essential differences with Ni and Fe are the following. There is an additional shift of electrons from the metal to the carbon atoms, especially for the μ_3 sites. (As pointed out in paper I, this shift in the Mulliken populations does not necessarily correspond with an increase in the work function of the system.) These electrons cause the occupied acetylene orbitals to have gross populations considerably larger than 2, suggesting a negative electron donation effect (see table 1). As discussed in section 3.1, this means in fact that there is a (strong) interaction between the occupied low lying metal orbitals and the occupied acetylene orbitals, an interaction which leads to the level splitting and broadening effects which we have just discussed. For the μ_3 sites mainly the acetylene π_u orbitals are involved, for the π and μ_2 sites (less strongly) the $3\sigma_g$ orbitals (see table 1); this corresponds with the presence of copper cluster orbitals with the correct symmetry, lying close in energy to the C_2H_2 orbitals concerned. This interaction between occupied orbitals, which dominates the electron donation effect, should have a net anti-bonding (repulsive) character; it will reduce the C_2H_2–metal bonding caused by the π^* back donation effect (the latter effect is still present on Cu). This may well explain the observation that C_2H_2 desorbs more readily from Cu than from Ni and Fe and does not dissociate [15,24].

Among the μ_3 sites, we notice that the charge shifts and the reduction of C–C overlap population is largest for the $\mu_3(b)$ sites, occurring on the (111) surface; this agrees with the relative π_u and $2\sigma_g$ level bonding shifts. Apparently the $\mu_3(a)$ site, where two of the metal atoms have a considerably larger distance ($a = b\sqrt{2}$) is less effective in interacting with C_2H_2 even though the Cu–C distances are the same (1.9 Å). A similar difference, albeit smaller, has been found for the μ_3 site on the Fe(110) surface as compared with the μ_3 site on Ni(111) (see section 3.1).

4. Conclusions

Summarizing the results of the previous sections, we can draw the following conclusions. Acetylene is bound to Fe surfaces via the Dewar–Chatt–Duncanson π to metal donation and metal to π^* back-donation mechanism [61,62]; the amount of back-donation is larger. Both effects weaken the acetylene C–C bond. No significant differences have been found between the more dense Fe surfaces and the Ni surfaces studied earlier; Fe as a bcc metal also has more open low index surfaces, however, which we have not investigated. The bonding on Cu surfaces is different. Here, the donation effect is dominated by an interaction between the occupied acetylene valence orbitals (mainly π_u and $3\sigma_g$) and the low lying occupied copper levels; the fact that occupied Cu orbitals (with the correct symmetry to interact with the C_2H_2 orbitals) are present in this energy range must be caused by the (filled) 3d band of copper lying lower than the (partly filled) 3d bands of Ni and Fe and by the bottom of the 4s band being lower as well for Cu [66–68] (these effects are represented already by some discrete levels in our very small metal

clusters). This relatively strong interaction between the occupied orbitals of nearly the same energy must cause an extra repulsion, which may well explain that the adsorption of C_2H_2 is weaker on Cu than on Ni and Fe. All these effects, donation, back-donation as well as repulsion, become more pronounced when the metal coordination of the acetylene bonding sites is higher: $\pi < \text{di-}\sigma < \mu_2 < \mu_3$. The μ_3 sites are most effective when the metal atoms are packed closer: $\mu_3 - \text{Cu}(100) < \mu_3 - \text{Cu}(111)$, $\mu_3 - \text{Fe}(110) \lesssim \mu_3 - \text{Ni}(111)$.

Our cluster calculations lead to an interpretation of some typical features in the observed UPS spectra for C_2H_2 adsorbed on Fe, Ni and Cu surfaces. The bonding shift of the π_u levels (relative to the $3\sigma_g$ level) is found in all cases, but the fact that Cu is exceptional by showing two distinct π_u peaks can also be explained by the calculations. This is caused by the strong interaction between the C_2H_2 valence orbitals and low lying copper orbitals (close in energy) which we have just discussed; the interaction leads to a splitting (and broadening) of the occupied levels. So, we suggest a relation between the extra peak in the UPS spectrum of C_2H_2 on Cu (observed both on the Cu(100) surface [15] and on Cu films [24]) and the weaker adsorption of C_2H_2 on Cu (as compared with Ni and Fe). Although the adsorption shifts in our calculated ionization energies are in fair agreement with the experimental UPS spectra we cannot determine from this comparison which are the preferred adsorption sites for C_2H_2 on Fe and Cu; the calculated ionization energy spectra for the different bonding sites show too small differences (also the experimental spectra are usually not very different if they have been measured on different single crystal surfaces [7,15,16,21,23] and on films [24]). We think that C_2H_2 adsorbs on Fe(110) in μ_2 or μ_3 positions and on the Fe(100) surface in μ_2 positions (see section 3.1). The extra information which was available for C_2H_2 on the Ni(111) surface (from the ELS spectrum [17,18,30]) is still lacking for Fe and Cu surfaces.

Acknowledgement

We thank Prof. Dr. P. Ros, Dr. E.J. Baerends and Dr. J.G. Snijders for making available the HFS–LCAO program.

The investigations were supported in part by the Netherlands Foundation for Chemical Research (SON) with financial aid from the Netherlands Organization for the Advancement of Pure Research (ZWO).

References

[1] H. Conrad, G. Ertl and E.E. Latta, Surface Sci. 41 (1974) 435.
[2] K. Christmann, U. Schokev, G. Ertl and M. Neuman, J. Chem. Phys. 60 (1974) 4528.
[3] K. Christmann, G. Ertl and T. Pignet, Surface Sci. 54 (1976) 365.

[4] M. Balooch, M.J. Cardillo, D.R. Miller and R.E. Stickney, Surface Sci. 46 (1974) 358.
[5] C. Backx, B. Feuerbacher, B. Fitton and R.F. Willis, Surface Sci. 63 (1977) 193.
[6] G. Brodén, T.N. Rhodin, C. Brucker, R. Benbow and Z. Hurych, Surface Sci. 59 (1976) 593.
[7] G. Brodén, G. Gafner and H.P. Bonzel, Appl. Phys. 13 (1977) 333.
[8] S.L. Bernasek and G.A. Somorjai, J. Chem. Phys. 62 (1975) 3149.
[9] R.J. Gale, M. Salmeron and G.A. Somorjai, Phys. Rev. Letters 38 (1977) 1027.
[10] D.G. Castner, B.A. Sexton and G.A. Somorjai, Surface Sci. 71 (1978) 519.
[11] K. Yoshida and G.A. Somorjai, Surface Sci. 75 (1978) 46.
[12] D.G. Castner and G.A. Somorjai, Surface Sci. 83 (1979) 60.
[13] J.E. Demuth and D.E. Eastman, Phys. Rev. Letters 32 (1974) 1123.
[14] J.E. Demuth, Surface Sci. 69 (1977) 365.
[15] J.E. Demuth, IBM J. Res. Develop. 22 (1978) 265.
[16] J.E. Demuth, Surface Sci. 84 (1979) 315.
[17] J.E. Demuth and H. Ibach, Surface Sci. 85 (1979) 365.
[18] J.C. Bertolini, J. Massardier and G. Dalmai-Imelik, JCS Faraday I, 74 (1978) 1720.
[19] J.E. Demuth and H. Ibach, Surface Sci. 78 (1978) L238.
[20] S. Lehwald and H. Ibach, Surface Sci. 89 (1979) 425.
[21] J.E. Demuth, Phys. Rev. Letters 40 (1978) 409.
[22] R. Mason and M. Textor, Proc. Roy. Soc. (London) A356 (1977) 47.
[23] C. Brucker and T. Rhodin, J. Catalysis 47 (1977) 214.
[24] K.Y. Yu, W.E. Spicer, I. Lindau, P. Pianetta and S.F. Lin, Surface Sci. 57 (1976) 157.
[25] S. Lehwald, W. Erley, H. Ibach and H. Wagner, Chem. Phys. Letters 62 (1979) 360.
[26] G. Casalone, M.G. Cattania, M. Simonetta and M. Tescari, Surface Sci. 62 (1977) 321.
[27] M.G. Cattania, M. Simonetta and M. Tescari, Surface Sci. 82 (1979) L615.
[28] J.C. Hemminger, E.L. Muetterties and G.A. Somorjai, J. Am. Chem. Soc. 101 (1979) 62.
[29] C.R. Brundle, Faraday Disc. 58 (1974) 138.
[30] J.C. Bertolini and J. Rousseau, Surface Sci. 83 (1979) 531.
[31] P. Geurts and A. van der Avoird, Surface Sci. 102 (1981) 185.
[32] A.B. Anderson, J. Am. Chem. Soc. 99 (1977) 696.
[33] T.N. Rhodin, C.F. Brucker and A.B. Anderson, J. Phys. Chem. 82 (1978) 894.
[34] J.E. Demuth and D.E. Eastman, Phys. Rev. B13 (1976) 1523.
[35] H. Itoh and A.B. Kunz, Chem. Phys. Letters 66 (1979) 531.
[36] E.J. Baerends, D.E. Ellis and P. Ros, Chem. Phys. 2 (1973) 41.
[37] E.J. Baerends and P. Ros, Chem. Phys. 2 (1973) 52.
[38] E.J. Baerends and P. Ros, Intern. J. Quantum Chem. S12 (1978) 169, and references therein.
[39] E. Clementi and C. Roetti, in: Atomic Data and Nuclear Data Tables, Vol. 14 (Academic Press, New York, 1974) p. 177.
[40] J.G. Snijders and E.J. Baerends, Mol. Phys. 33 (1977) 1651.
[41] R.C. Weast, Ed., Handbook of Chemistry and Physics, 55th ed. (CRC Press, Cleveland, 1974) pp. F-200, 201.
[42] H.C. Allen, Jr. and E.K. Plyder, J. Am. Chem. Soc. 80 (1958) 2673.
[43] K. Nicholas, L.S. Bray, R.E. Davis and R. Pettit, Chem. Commun. (1971) 608.
[44] H.J. Schmitt and M.L. Ziegler, Z. Naturforsch. 28b (1973) 508.
[45] F.A. Cotton, J.D. Jamerson and B.R. Stults, J. Organometal. Chem. 94 (1975) C53.
[46] R.P. Dodge and V. Schomaker, J. Organometal. Chem. 3 (1965) 274.
[47] J.F. Blount, L.F. Dahl, C. Hoogzand and W. Hübel, J. Am. Chem. Soc. 88 (1966) 292.
[48] E. Sappa, A. Tiripicchio and M. Tiripicchio Camellini, JCS Dalton (1978) 419.
[49] F.A. Cotton, J.D. Jamerson and B.R. Stults, J. Am. Chem. Soc. 98 (1976) 1774.
[50] W.G. Sly, J. Am. Chem. Soc. 81 (1959) 18;
see also ref. [9] in D.A. Brown, J. Chem. Phys. 33 (1960) 1037.

[51] L.F. Dahl and D.L. Smith, J. Am. Chem. Soc. 84 (1962) 2450.
[52] R.S. Dickson and J.A. Ibers, J. Organometal. Chem. 36 (1972) 191.
[53] Y. Wang and P. Coppens, Inorg. Chem. 15 (1976) 1122.
[54] O.S. Mills and B.W. Shaw, J. Organometal. Chem. 11 (1968) 595.
[55] V.W. Day, S.S. Abdel-Meguid, S. Dabestani, M.G. Thomas, W.R. Pretzer and E.L. Muetterties, J. Am. Chem. Soc. 98 (1976) 8289.
[56] J.L. Davidson, M. Green, F.G.A. Stone and A.J. Welch, J. Am. Chem. Soc. 97 (1975) 7490.
[57] M.G. Thomas, E.L. Muetterties, R.O. Day and V.W. Day, J. Am. Chem. Soc. 98 (1976) 4645.
[58] J.C. Slater, Quantum Theory of Molecules and Solids, Vol. 4 (McGraw-Hill, New York, 1974).
[59] R.S. Mulliken, J. Chem. Phys. 23 (1955) 1833.
[60] R.S. Mulliken, J. Chem. Phys. 23 (1955) 1841.
[61] M.J.S. Dewar, Bull. Soc. Chim. France 18 (1951) C79.
[62] J. Chatt and L.A. Duncanson, J. Chem. Soc. (1953) 2939.
[63] D.W. Turner, C. Baker, A.D. Baker and C.R. Brundle, Molecular Photoelectron Spectroscopy (Wiley, London, 1970).
[64] E.J. Baerends and P. Ros, Mol. Phys. 30 (1975) 1735.
[65] D.E. Ellis, E.J. Baerends, H. Adachi and F.W. Averill, Surface Sci. 64 (1977) 649.
[66] H. Ehrenreich and L.M. Schwartz, Solid State Phys. 31 (1976) 149.
[67] V.L. Moruzzi, J.F. Janak and A.R. Williams, Calculated Electronic Properties of Metals (Pergamon, New York, 1978).
[68] M. Mehta and C.S. Fadley, Phys. Rev. B20 (1979) 2280.